Applied Energy xxx (2016) xxx–xxx

Contents lists available at ScienceDirect

Applied Energy

journal homepage: www.elsevier.com/locate/apenergy

The cooling performance of a natural draft dry cooling tower under crosswind and an enclosure approach to cooling efficiency enhancement

Weiliang Wang [a,b], Hai Zhang [a], Pei Liu [a,*], Zheng Li [a], Junfu Lv [a], Weidou Ni [a]

[a] State Key Laboratory of Power System, Department of Thermal Engineering, Tsinghua-BP Clean Energy Center, Tsinghua University, Beijing 100084, PR China
[b] Guodian Science and Technology Research Institute, Nanjing 210046, PR China

HIGHLIGHTS

- The cooling performance of a NDDCT under crosswind condition was investigated.
- The resistance of radiators was simulated using a viscous force based equation.
- A gentle breeze or stronger wind may influence the cooling performance of a NDDCT.
- Vortices and circumferential non-uniformity are the main degrading factors.
- An enclosure approach to cooling efficiency enhancement is found to be effective.

ARTICLE INFO

Article history:
Received 14 September 2015
Received in revised form 30 January 2016
Accepted 2 February 2016
Available online xxxx

Keywords:
NDDCT
CFD
Indirect dry cooling
Crosswind
Enclosure
Performance enhancement

ABSTRACT

Cooling performance of a natural draft dry cooling tower degrades in presence of crosswind. Upon an in service natural draft dry cooling tower of a 660 MW unit in China, a computational fluid dynamics approach with validation is adopted to investigate the cooling performance at various wind speeds. The first order viscous force based resistance mechanism is used in simulating the air flow resistance for the radiators. Numerical results confirm previous findings that the cooling performance of the natural draft dry cooling tower degrades with the increment of wind velocity when wind velocity is higher than 4 m/s, but the performance reduction is relatively less. The circumferential non-uniform ventilation and the vortices inside the tower contribute the most to the degrading of the cooling performance when crosswind is present. To enhance the overall cooling performance, an enclosure with an opening at the windward side is proposed to increase the pressure level outside the side and back radiators. Numerical results show that such an enclosure could enhance the cooling performance at all investigated wind speeds, with 36% increase of the ventilation rate and about 7 °C decrement of the cycling water temperature at 20 m/s.

1. Introduction

The power plants consume approximately half the global industrial water withdrawal [1]. As an effective water saving technology, indirect dry cooling technology has been increasingly used in the recent years for the power generation in arid countries and regions, for its merits of low noise, long service life, simple maintenance and high energy saving [2,3]. However, it was found the efficiency of dry cooling is sensitive to the ambient crosswind and weather fluctuation, which could introduce a maximum output variation in the range of 5–10% of the nominal capacity in intraday operation [4]. It is of great significance if the ambient crosswind could be positively used rather than negatively affecting the power generation efficiency.

Nowadays, some studies on ambient crosswind utilization have been conducted on the natural draft dry cooling tower (NDDCT), the primary structure of indirect dry cooling system. Through experimental research, Wei et al. [5] found that crosswind at speed of 6 m/s reduce the mean velocity rate along the annular radiators about 20%; Cui and Lu [6] reported that the influences of crosswind at speed of 5 m/s and 15 m/s equal to those of about 2 °C and 14 °C rises of the environmental temperature; Lu et al. [7] argued that the total heat transfer rate of a NDDCT is a combination of natural convective heat transfer and forced convective one, and depending on their ratio, a turnabout point wind speed exists, below which the heat transfer decreases with increasing crosswind speed and

* Corresponding author. Tel.: +86 (010) 627 957 34; fax: +86 (010) 627 957 36.
E-mail address: liu_pei@tsinghua.edu.cn (P. Liu).

http://dx.doi.org/10.1016/j.apenergy.2016.02.007
0306-2619/

Nomenclature

error	the error between simulation results and reference data (°C)
$\vec{g}$	gravity acceleration vector (m/s^2)
h	heat transfer coefficient (W m^{-2} K^{-1})
ITD	initial temperature difference between the cycling water and environment (K)
k	turbulent kinetic energy (J)
M	momentum source term (kg m^{-1} s^{-1})
NDDCT	natural draft dry cooling tower
P	pressure (kPa)
Q	the overall heat released from the radiators (MW)
q	constant energy source term (W m^{-3})
R	equivalent resistance coefficient (%)
S_{ij}	the tensor of strain rate
T	temperature (K)
u	velocity scalar (m s^{-1})
$\vec{V}$	velocity vector (m s^{-1})

Greek letters

∇	Hamiltonian
μ	dynamic viscosity (N s m^{-2})
a	permeability (m s^{-1})
β	air compressibility coefficient
ε	turbulent dissipation
ρ	air density (kg m^{-3})

Subscripts

a	environmental air parameter
bottom	bottom part of the tower
chamber	tower chamber part
h	high terminal value
l	low terminal value
radiator	radiators section value
ref	reference data
s	source term
Sim	simulation results
t	turbulent parameters
total	total value of the tower

above which it does the reverse. More recently, more computational fluid dynamics (CFD) simulation were carried out. Zhao et al. [8] found that crosswind at speed of 5 m/s and 10 m/s raises the cycling water outlet temperature by 1 °C and 5 °C respectively. Zhang and Wang [9] found that crosswind at speed of 4 m/s, 6.6 m/s and 8.5 m/s degrades the cooling capacity by 5%, 10% and 25% respectively. Al-Waked and Behnia [10] found that crosswind speed at higher than 10 m/s degrades the thermal effectiveness by more than 30% (at constant ejected temperature). Goudarzi [11] found that the reduction of cooling efficiency could be up to 35% at the crosswind speed of around 18 m/s. Yang et al. [12] found that reduction of mass flow rate of the cooling air reaches its peak at around 40% at crosswind speed of 12 m/s. Zhao et al. [13] confirmed the findings and revealed that the reduction of cooling air could be up to 45%, and further found that the turnabout point is postponed to 16 m/s under constant heat load condition (while the previous study is under set water temperature condition) [14]. Based on the existing researches, we can see that crosswind effect becomes obvious from 4 m/s and the cooling capacity may decline 30–45%.

Typically, a NDDCT has three parts of effective chimney: heat exchanger bundle, plenum chamber, and the effective plume part [15,16]. As found by Wei et al. [5], crosswind affects the cooling efficiency of a NDDCT by three ways: (a) The wind forms an unfavourable pressure distribution at the tower inlet (heat exchanger part); (b) The wind disturbs the hot plume rising from the cooling tower (plume part); (c) The wind causes the back flow induced by the separation vortex at the leading edge of the tower outlet (plenum chamber part). Tang et al. [17] found that crosswind lead to a horizontal air flow in the tower to degrade the upward flow, even a cross ventilation at a high wind speed, which might degrade the heat transfer in side and rear (plenum chamber and heat exchanger parts). Zhai et al. [18,19] found that inlet air flow from the leading and rear radiators converge to produce complex vortices, hindering the upward flow and side/rear air inlet (plenum chamber and heat exchanger parts). Zhang et al. [20] and Goodarzi [21] both reported that crosswind squeezes the plume flow, leading to smaller outlet cross section and higher flow resistance along the path line (plume part). Besides, Bergles [22], Zhai and Fu [23] also reported that the suck-back of cold air at the outlet of the tower would also affect the flow field in the tower. Fisher and Torrance [24] found that the such-back of cold air at the outlet of small heat exchangers might degrade the thermal efficiency by 4%.

In order to reduce the negative crosswind effect on NDDCT, many ideas were reported in 1970 s and 1980 s, including dry/wet associated cooling, plastic tower shell, periodic dry cooling, etc. [25,26], but rather rare afterward. In 1993, wind-breaks was first proposed by Du Preez and Kroger [27], and then verified by Al-Waked and Behnia [10,28] and Zhai and Fu [23] through numerical investigation. Dai et al. [29] and Wang [30] revealed that guiding channel could promote the cooling performance of a natural draft wet cooling tower (NDWCT), by 5–10%. Later, Zhao et al. [31] and Chen et al. [32] found that the cross-wall could enhance the cooling efficiency of a NDWCT at lower crosswind speeds, but sensitive to wind direction at higher speeds, through numerical and experimental study respectively. Goodarzi [21] proposed a new inclined exit configuration to improve the cooling efficiency by 9% at 10 m/s crosswind. More recently, Lu et al. [33] found that in-tower windbreaks could reverse the negative crosswind effect to positive in a small NDDCT, at certain wind attack angles. Goodarzi et al. [34,35] reported that windbreaks constructed as radiators could even promote the cooling efficiency in NDDCT, and an elliptical cross section type cylinder could improve the cooling efficiency by 17% at 10 m/s crosswind speed.

Crosswind is generally regarded as a power source commonly used in architecture field, like wind tower [2] and wind catches [36], even to achieve nearly net zero energy buildings [37]. These applications imply that crosswind could also be used to improve the thermal performance of cooling towers. Thus, this paper presents an enclosure structure with an opening at the windward side located outside the heat exchanger bundle, to assess the flexibility to use the wind potential for the cooling efficiency improvement. Given the influence on cooling efficiency of a NDDCT by the crosswind is mainly attributed to the change of the ventilation rate, the study focuses on the assessment of the ventilation of the tower and the fluid dynamics in the air side, and then evaluate the overall performance with empirical data.

Please cite this article in press as: Wang W et al. The cooling performance of a natural draft dry cooling tower under crosswind and an enclosure approach to cooling efficiency enhancement. Appl Energy (2016), http://dx.doi.org/10.1016/j.apenergy.2016.02.007

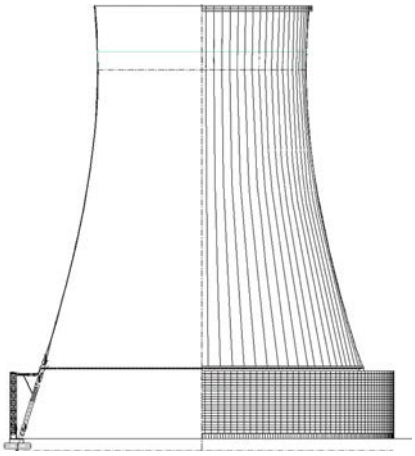

(a): An overview of the NDDCT

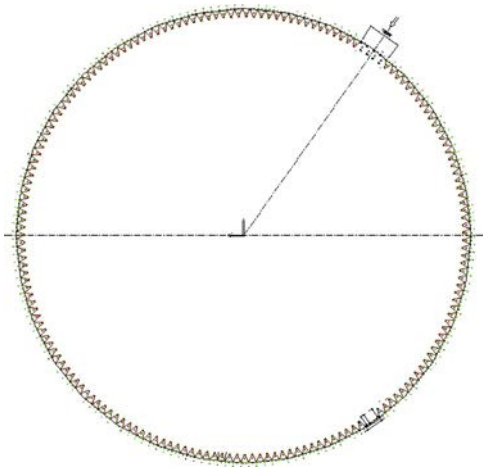

(b): The distribution of cooling deltas

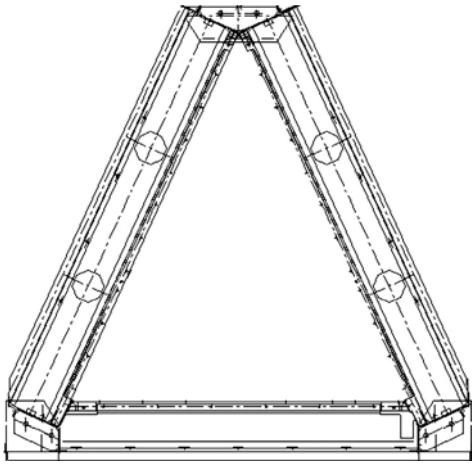

(c): The cross section of a cooling delta

Fig. 1. Schematic of a typical NDDCT.

2. Methods

2.1. Problem description

A typical NDDCT schematic is shown in Fig. 1(a), which is of Heller type commonly used in 660 MW dry cooling power plants in China. The NDDCT has a total height of 170 m, a tower bottom height of 27.5 m, a base radiator height of 24 m, a radiator support of 2 m, an outlet diameter of 84.466 m, a throat diameter of 82 m, and a base radiator diameter of 146.17 m. Fig. 1(b) shows the schematic of cooling deltas distribution and cooling section division, which has 183 deltas and 10 sectors nearly equally distributed on the bottom of the tower, except one part where a flue gas pipe is induced from outside to inside at the up-right part. Fig. 1(c) shows the schematic of a cooling delta cross section, which has two vertical cooling columns shown as the two sides of the triangle. Each cooling column is composed of 4 pieces of radiators. Each piece of radiator has a bundle of 80 × 6 staggered tubes, with a height of 6 m, a width of 2.408 m and a thickness of 0.15 m. The spacing between adjacent fins is 3.1 mm.

Warm cycling water flows through the staggered tubes, and then cooled down by the ambient air outside. The water is used to condense exhaust steam from the exit of low pressure cylinder. The cooling air is then heated by the cycling water and becomes lighter in density. Finally the natural draft is generated by the density difference between the air inside and outside of the tower, making the cooling air continuously flow from the cooling deltas. When crosswind is present, the flow fields around the cooling deltas, inside of the tower and tower outlet are changed, reducing the

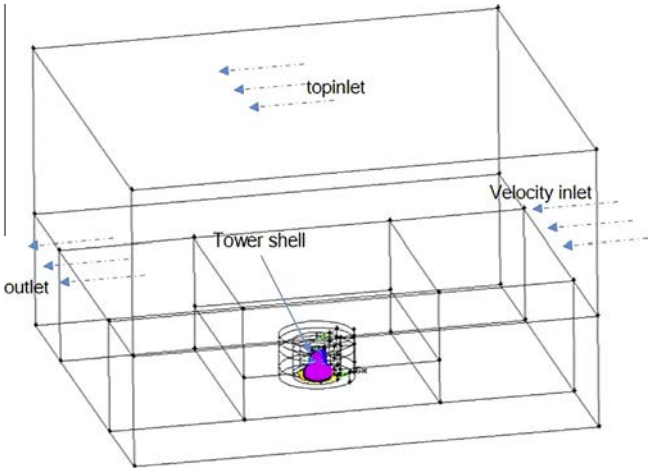

Fig. 2. Schematic of the computational field and its boundaries for air flow in the presence of crosswind.

Please cite this article in press as: Wang W et al. The cooling performance of a natural draft dry cooling tower under crosswind and an enclosure approach to cooling efficiency enhancement. Appl Energy (2016), http://dx.doi.org/10.1016/j.apenergy.2016.02.007

ventilation rate, and thereby degrade the cooling effect of the tower.

2.2. Computational field

The computational field in Fig. 2 has a dimension of 2764 m × 2512 m × 1700 m, which is large enough compared with the tower size (more than 10 times in directions of x, y and z respectively) to eliminate the unrealistic effect of the domain boundaries on the flow field crosswind outside and inside the tower. The structure of the cooling deltas, tower shells, the support and joint faces between adjacent radiators are all constructed in strict accordance with the real case. The enclosure added to the outside of the cooling deltas is schematically shown in Fig. 3, which is about 220 m in radius and 62 m in height, especially designed large enough to avoid disturbing the airflow on wind free condition. The computational meshes are generated with the commercial software Gambit [38]. Hexahedral structured grids are used in the computational domain except one joint field 50 m above the top of the tower. The grid interval size is about 0.15–0.3 m near the heat exchanger, and about 1–2 m near the tower shell. However it is about 20 m near the inlet and outlet of the computational field. In the domain far from the central part, the grid interval size adopts the successive ratio grading scheme instead of the uniform division, so that fewer meshes are generated to meet the computational demands. At the transition points between the surfaces or volumes, the meshes are smoothed manually by adjusting the edges/surfaces grid size.

2.3. Boundary conditions and basic assumptions

Although many researches tend to study the cooling performance of NDDCT by solving the conjugate fluid–solid–fluid heat transfer problems among the air, radiators, and cycling water and fluid dynamics problems in the air side simultaneously [10,12,13,35,39], the modelling of fluid flow and heat transfer under coupled conditions remains a challenging issue particularly for industrial-scale systems [40]. Provided that the knowledge that the change of water vaporization latent heat is negligible within the common back pressure [14,41,42], the heat release from the condenser and thereby heat dissipation from the radiators is constant. Using the correlation between the heat transfer coefficient and air velocity presented by Yang et al. [12], we can calculate the ITD (initial temperature difference) based on the energy conservation formula and the corresponding boundary conditions. Consequently, the radiators are simplified as a constant heat source, and the crosswind effect can be described by the ventilation rate of the NDDCT instead of its ITD or other parameters. The temperature change of the cycling water can be calculated based on given heat transfer mechanism.

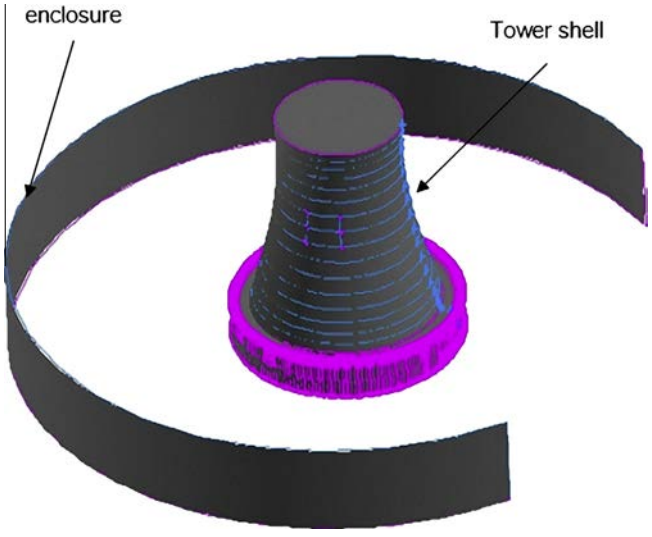

Fig. 3. Schematic of the enclosure and its opening.

Generally the wind velocity is a function of height above the ground, and its profile may affect the crosswind effect [10], while it tends to be unchanged when the height is above 10 m. Since the dimension of the radiators and computational field are relatively large, the crosswind is assumed to be constant at the inlet. At the downstream surface both upward and rearward, the outflow boundary is appointed due to the unchanging velocity and temperature profiles. On the other surfaces like the side surfaces, the ground, the inside/outside cooling tower shells and the support and joint faces between adjacent radiators are all set as adiabatic wall conditions with no slip condition. The pressure-based solver in Fluent with pressure–velocity coupling SIMPLEC method is used. The governing equations of the momentum, energy, turbulent kinetic energy and dissipation rate are discretized using the second-order upwind differencing scheme [38].

2.4. Governing equations

The flow regime is turbulent, and air density variation in the cooling tower is so small that the flow can be assumed incompressible and Boussinesq approximation can be used in the vertical momentum equation to consider the buoyancy force [35]. Governing equations for steady, buoyant, and turbulent flow including heat transfer are continuity, momentum, energy, and turbulence modelling equations, as shown in Eqs. (1)–(5). The well-known standard k–ε model is used to model the turbulent flow.

$$\vec{\nabla}\cdot\vec{V} = 0.0 \tag{1}$$

$$\rho(\vec{V}\cdot\vec{\nabla})\vec{V} = -\vec{\nabla}p + \vec{\nabla}\tau - \rho\beta(T - T_{ref})\vec{g} + \vec{M}_s \tag{2}$$

$$\rho(\vec{V}\cdot\vec{\nabla})T = -\vec{\nabla}[(\Gamma + \Gamma_t)\vec{\nabla}T] + q_s \tag{3}$$

$$(\vec{V}\cdot\vec{\nabla})k = \vec{\nabla}\left[\left(\nu + \frac{\nu_t}{\sigma_k}\right)\vec{\nabla}k\right] + P + G - \varepsilon \tag{4}$$

$$(\vec{V}\cdot\vec{\nabla})\varepsilon = \vec{\nabla}\left[\left(\nu + \frac{\nu_t}{\sigma_\varepsilon}\right)\vec{\nabla}\varepsilon\right] + C_{1\varepsilon}\frac{\varepsilon}{k}(P + G) - C_{2\varepsilon}\frac{\varepsilon^2}{k} \tag{5}$$

in which $\tau_{ij} = (\mu + \mu_\tau)S_{ij}$, $P = \nu_\tau S_{ij}S_{ij}$, $G = -g\beta\frac{\nu_\tau}{\sigma_\tau}S_{ij}\frac{\partial T}{\partial Z}$, $S_{ij} = \frac{1}{2}\left(\frac{\partial V_i}{\partial x_j} + \frac{\partial V_j}{\partial x_i}\right)$, $\nu_\tau = \frac{\mu_\tau}{\rho} = C_\mu\frac{k^2}{\varepsilon}$, $\Gamma = \frac{\mu}{Pr}$, $\Gamma_t = \frac{\mu_t}{Pr_t}$, and, $C_\mu = 0.09$, $C_{1\varepsilon} = 1.44$, $C_{2\varepsilon} = 1.92$, $\sigma_k = 1.0$, $\sigma_\varepsilon = 1.3$, $\sigma_t = 1.0$ are constant of standard k–ε equations. In the above equations $\vec{V}$, P, ρ, μ and μ_t are velocity vector, static pressure, air density, molecular viscosity, and turbulent viscosity, respectively; T and T_{ref} are local and reference temperatures, respectively; β denotes the air compressibility coefficient; $\vec{g}$ is gravity acceleration vector, and S_{ij} is the tensor of strain rate.

Each cooling triangle is composed of 4 pieces of heat exchangers, which adopts an advanced forgo type aluminium H-fins heat sink. So far, a number of studies have been conducted on heat transfer enhancement [43–48]. In the present study, the air flow and heat transfer between the radiators' fins are simplified by using a porous medium model in the region where the radiator is located. There are merely additions of a momentum source term and a heat source term to the standard flow Eq. (2) and energy Eq. (3) in this region [38,49]. As the flow regime in the radiator is

Please cite this article in press as: Wang W et al. The cooling performance of a natural draft dry cooling tower under crosswind and an enclosure approach to cooling efficiency enhancement. Appl Energy (2016), http://dx.doi.org/10.1016/j.apenergy.2016.02.007

Table 1
Ventilation capacity at different grids number (kg/s).

Grids number	7,535,281	8,354,613	12,268,096	13,371,319
V_a = 0.5 m/s	36,251	36,220	36,214	36,201
V_a = 4 m/s	36,584	36,603	36,664	36,670

laminar (Re < 540), the pressure drop is proportional to the flow velocity and the inertial flow loss in the radiator can be omitted. Ignoring convective acceleration and diffusion, the momentum source term $\vec{M}$ is written as

$$\vec{M}_s = \nabla p = -\frac{\mu}{a}\vec{v} \tag{6}$$

For an orthotropic fill resistance in the finned-tube radiator cores, the oblique flow entering the fill is forced into the horizontal direction by the radiator fins. This change of direction can be modelled by means of the anisotropic porous medium model by making vertical loss coefficients in Eq. (6) very large to simulate the impermeability of the fins in that direction [49].

As the overall heat transfer between the radiators and inlet air flow is simplified as an addition of a constant energy source term of q_s to the standard energy Eq. (3) in this region. In the interested nominal condition,

$$q_s = 258234.7\ \mathrm{W/m^3} \tag{7}$$

To calculate ITD, the convective heat transfer coefficient h can be specified as the following form.

$$h = \sum_{n=1}^{3} h_n u^{n-1} \tag{8}$$

where u is the local surface velocity, and h_n is the polynomial coefficient, calculated as h_1 = 1451.95, h_2 = 1156.59, h_3 = −75.615 in terms of the convective heat transfer experimental data through the finned tube bundles [12].

2.5. Validations

Table 1 shows the grid checking results of numerical simulation on the performance of NDDCT. Meshes of 7,535,281, 8,354,613, 12,268,096 and 13,771,319 cells at the crosswind speed of 0.5 m/s and 4 m/s are checked respectively. The ventilation rate (mass flow rate) at the same boundary condition varies slightly with the increase of grid number, by 0.16% at the most, and only about 0.036% and 0.016% between the two grid number of 12,268,096 and 13,371,319. Thus, the mesh with the grid number of 13,771,319 is chosen for its better assessment and convergence.

In order to further verify the CFD model, we chose two design data and two experimental data as the reference cases, as shown in Table 2. The ITD of the cooling air under design and experimental conditions are denoted as ITD_{ref}. The experiments were carried out right after the unit's first 168 h operation, and the ITD_{sim}s were calculated based on the calculated total mass flow rate of the tower, specific flow resistance, reference average temperature difference, and reference cycling water decrease, as showed in Eq. (9). The boundary conditions and calculated total mass flow rate are also shown in Table 2. From Table 2 we can see that the calculated ITD_{sim}s are about 2.5% larger than the design data, and about 0.9% larger than the measured data. The results confirm the validity of the CFD numerical model.

$$ITD_{sim} = t_{sim-h} - T_{sim-h} = \frac{T_{ref-h} - T_{ref-l}}{2}\frac{q_{ref}}{q_{sim}} + \frac{(t_{ref-h} - T_{ref-h}) + (t_{ref-l} - T_{ref-l})}{2}\frac{h_{ref}}{h_{sim}} - \frac{t_{ref-h} - t_{ref-l}}{2} \tag{9}$$

3. Results & discussion

3.1. Crosswind effect on NDDCT

Under wind free condition, the cooling air enters the tower uniformly through the vertical arranged radiators on the bottom of the tower, and heated by the cycling water inside the radiators, resulting in a natural draft of the cooling tower. The flow field of the vertical parting surface of the NDDCT under four typical crosswind conditions are illustrated in Fig. 4, in which the colour ranging from blue to red represents the velocity magnitude ranging from 0 to 25 m/s. From Fig. 4(a) we can find a small vortex stuck to the inner wall at the bottom section of the tower shell (named as *inner wall vortex*) as the result of the air current steering inside the tower under wind free condition, which has not been found in previous studies. As the increment of the velocity of the crosswind, the symmetric flow field inside the tower is destroyed; the inner wall vortex at the windward side grows greatly; and the plume at the outlet of the tower is suppressed to deflect to the backward of the tower as shown in Fig. 4(b)–(d), which is in consistent with the findings of Zhang et al. [20] and Goodarzi [21]. When the crosswind grows to be strong breeze (12 m/s), another vortex arises inside the outlet of the tower at the windward side to suck-back the cold air depicted in Fig. 4(b), which is also reported by Bergles [22] and Zhai and Fu [23]. Besides, vortices at the back of the tower are found under most crosswind conditions, and become more complex as the crosswind velocity increases.

The flow fields of the horizontal cross section inside the radiators at four typical crosswind velocities are shown in Fig. 5. The unbalanced inward air flows at the windward side and the leeward side induce two symmetric vortices (named as *mainstream vortices*) when the crosswind velocity is higher than 4 m/s. As the crosswind grows stronger, the two vortices gradually separate apart from the centre of the tower to the back and side, and grows bigger and stronger. Fig. 5(c)–(d) shows that the maximum swirling velocities of the two vortices may exceed that of the inward air flow at the windward side when crosswind velocity is higher than 10 m/s, leading to a great ventilation barrier to the radiators in the back and side sections, consistent to the results of Zhai et al. [18,19]. When the crosswind becomes a fresh gale (20 m/s), the horizontal air flow inside the radiators becomes a cross ventilation, as reported by Tang et al. [17].

The pressure contours in a horizontal cross plane at the middle of the radiators at four typical velocities are exhibited in Fig. 6 respectively, in which the blue colour represents low pressure

Table 2
Validation of the CFD model with experimental and design data.

	Q (MW)	V_a (m/s)	T_a (°C)	P_a (kPa)	ITD_{ref} (kg/s)	ITD_{sim} (kg/s)	$Error_{ITD}$ (°C)
Design case 1	816.6	4.00	33.00	92.70	31.50	31.59	0.09
Design case 2	791.1	4.00	15.30	92.70	31.75	31.23	−0.52
Experimental case 1	827.7	1.97	27.36	94.02	30.418	30.174	−0.244
Experimental case 2	773.16	3.47	25.22	93.87	29.341	28.992	−0.349

Please cite this article in press as: Wang W et al. The cooling performance of a natural draft dry cooling tower under crosswind and an enclosure approach to cooling efficiency enhancement. Appl Energy (2016), http://dx.doi.org/10.1016/j.apenergy.2016.02.007

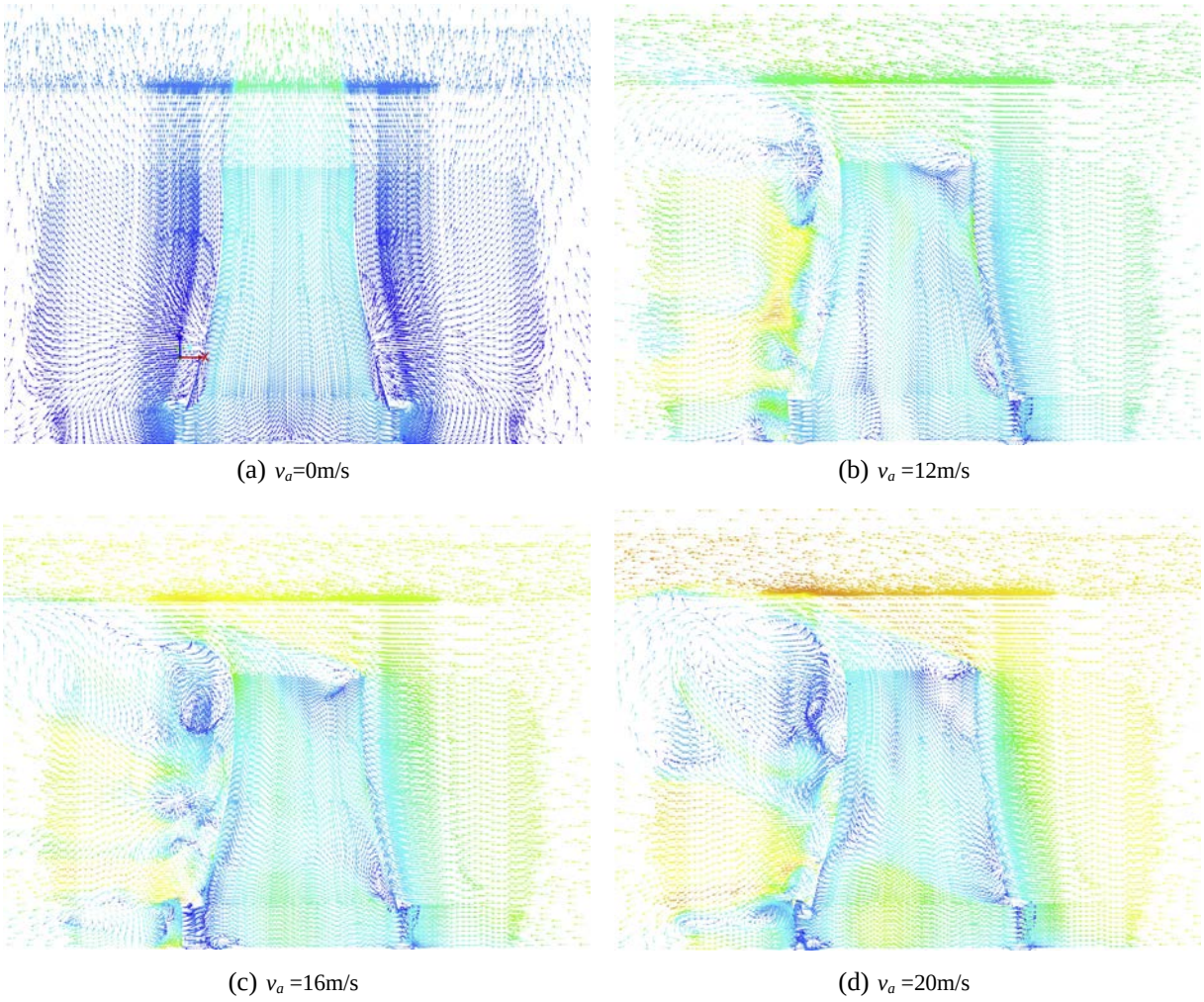

(a) v_a=0m/s (b) v_a =12m/s

(c) v_a =16m/s (d) v_a =20m/s

Fig. 4. The flow field of the vertical parting surface of the base NDDCT.

and red colour represents high pressure. Obviously, the pressure distribution becomes asymmetry as crosswind velocity exceeds 4 m/s. With the increasing of crosswind speed, the windward pressure outside the radiators increases gradually, and the side pressure outside the radiators decreases gradually. At the crosswind velocity of 14 m/s, the pressure outside the side radiators is found to be lower than that inside the radiators, indicating that the heated air inside the tower would be sucked out through the radiators at the side sections. This is extremely harmful to the cooling of cycling water inside the radiators. As the crosswind rises to 18 m/s, the pressure inside the back side radiators is found to be higher than that outside the radiators, which corresponds to the cross ventilation phenomenon discussed in the last paragraph. These unfavourable pressure distributions outside and inside the radiators induced by the crosswind greatly degrade the cooling performance of a NDDCT.

Fig. 7 depicts the circumferential distributions of the mass flow rate of cooling air through radiator sections at three typical crosswind velocities, in which the positive value indicates that the cooling air enters the tower from outside, whilst the negative value indicates that the air flows out from the inside of the tower. It can be drawn that, generally the mass flow rate at windward sections (from 0° to around 50° and from around 310° to 360° in this case) increases with the increment of crosswind velocity, whilst the mass flow rate at side and back sections (from around 50° to 310° in this case) decreases with the increment of crosswind velocity. Side sections suffer the ventilation degradation most severely at most cases. When the wind velocity increases to 14 m/s, a negative value of the mass flow rate at side section is found, which justifies the discussion in the last paragraph that the heated air is sucked out in this area. When the wind velocity rises to 18 m/s, a negative value of mass flow rate is also found at the back side section, which further justifies the conjecture in the last two paragraphs that the cross ventilation exists in fresh gale condition.

The cooling performance of the interested NDDCT is studied under crosswind velocities varying from 0 m/s to 20 m/s. The overall ventilation mass flow rate of the tower and ITD under different crosswind conditions are illustrated in Fig. 8, in which the ITD is calculated based on Eq. (9). From Fig. 8 we can infer that the crosswind takes effect at a velocity from around 4 m/s, resulting in a slight cooling performance degradation; as the velocity rises, the ventilation rate decreases with an increasing rate, whilst the ITD increase in the opposite way. At the 10 m/s speed crosswind of most researchers' attention, the ventilation rate is found to be reduced by 13.3%, and the ITD is increased by 2.65 °C; and at the 20 m/s, highest speed of this paper's interest, the ventilation rate is reduced by 40.4%, and the ITD is increased by 11.6 °C. Compared to the published results, the result confirms that the crosswind does degrade the cooling efficiency of NDDCT. However, the degradation degree of the cooling performance under gentle breeze conditions (below 5 m/s) shown in Fig. 4 is in consistent with many

Please cite this article in press as: Wang W et al. The cooling performance of a natural draft dry cooling tower under crosswind and an enclosure approach to cooling efficiency enhancement. Appl Energy (2016), http://dx.doi.org/10.1016/j.apenergy.2016.02.007

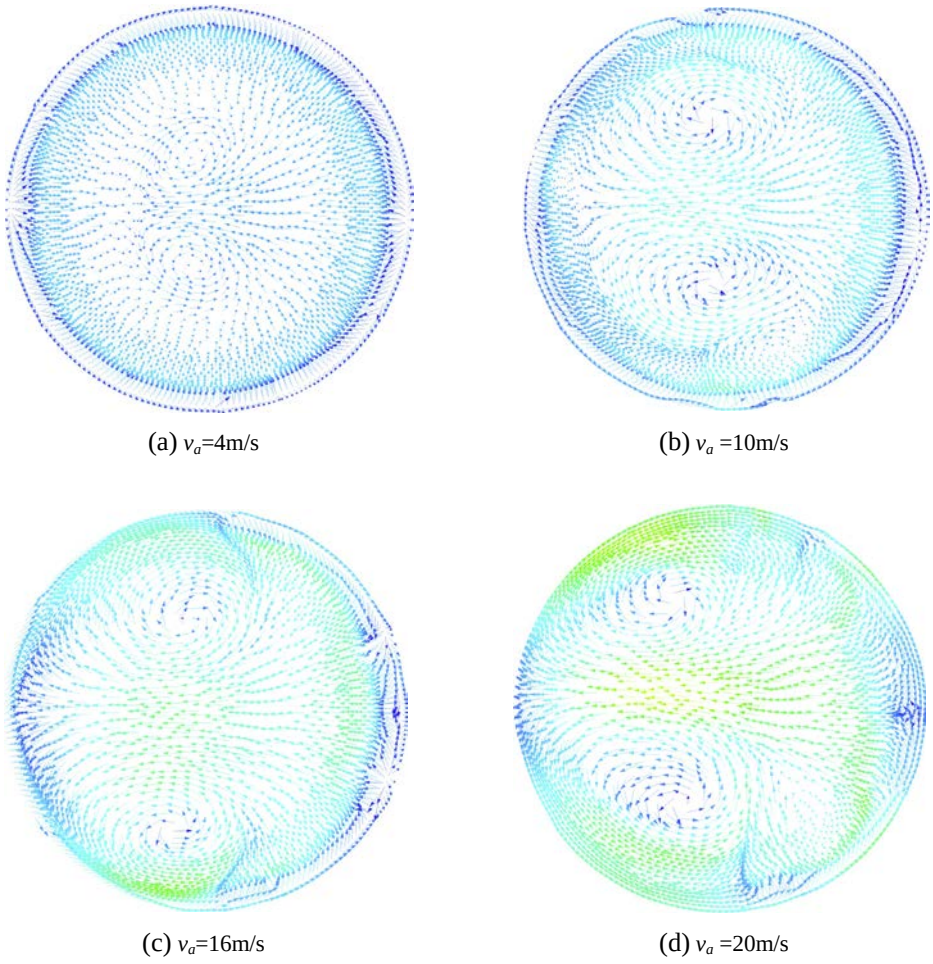

(a) v_a=4m/s (b) v_a =10m/s

(c) v_a=16m/s (d) v_a =20m/s

Fig. 5. The flow field of the horizontal cross section inside the radiators of the base NDDCT.

published experimental results listed in [5,6,8], but it is relatively lower than many published results in [10–13,20], whose claims are around 28%, 27%, 33%, 44% and 20%, at around 10 m/s. Besides that, no turnabout point is found as argued in [5,12,13], whose reported turnabout crosswind velocity are 6 m/s, 12 m/s and 12 m/s respectively. By comparing the boundary conditions with the previous study, there are mainly two important factors may accounting for this results. One factor is that the resistance mechanism at the radiator field adopted in this study is one order viscous force based resistance mechanism as explained in Eq. (6), which benefits the air flow in high local speed conditions. Another reason is that the resistance coefficient set in this simulation is relatively larger, which results in a lower ventilation rate (36,109 kg/s in nominal condition verified by design and experimental data), compared to around 94,500 kg/s in L. Yang's study [12], and 220,000 kg/s in Y. Zhao's study [13], and this may reduce the sensibility to crosswind.

In order to investigate the influencing mechanism of the crosswind quantitatively, we choose four pressure surfaces along the path line of the cooling air as shown in Fig. 9, and study the resistance property of the flow fields between the pressure surfaces. In Fig. 9, the surface out of the radiators represents the inlet cross section of the annular path of the radiators field, the surface inside the radiators delegates the outlet cross section of the annular path of the radiators field; the inlet surface of the tower chamber refers to the horizontal cross section right above the radiators bundle section; and the outlet surface of the tower chamber refers to the cross section of the tower outlet. The pressure losses between each couple of pressure surfaces are first extracted to their root, and then transferred to a hundred mark coefficient on the basis of same ventilation rate as exhibited in Fig. 10 (named as relative root resistance coefficient, Rrr for short), in which Rrr-radiator Rrr-bottom, Rrr-chamber and Rrr-total represent the relative root resistances of the radiators section, bottom section between the surface inside the radiators and the inlet surface of the tower chamber, plenum chamber part, and their summation respectively.

With the transformation of the pressure loss to be Rrr, it can be drawn from Fig. 10 that the Rrr-total has a similar variation trends as that of ITD, which represents the cooling performance of the NDDCT. The variation trend of Rrr-chamber shows that the resistance increment in the plenum chamber dominates the degradation of the NDDCT's cooling performance under moderate breeze and below crosswind conditions, and as the rise of the crosswind velocity, the flow resistance in this field gradually becomes favourable above strong breeze condition, probably as the result of the squeezed effective flow area due to side deviation of the swirling flow under low speed crosswind conditions and extended effective flow area due to the strong swirling flow under high speed crosswind condition. The variation trend of the Rrr-radiator exhibits an opposite way of the Rrr-chamber, probably as the result of the non-uniform characteristics of the air inlet through the radiators. The variation trend of Rrr-bottom directly conveys the complexity of the flow characteristics including vortices, horizontal ventilation, and asymmetry flow.

Please cite this article in press as: Wang W et al. The cooling performance of a natural draft dry cooling tower under crosswind and an enclosure approach to cooling efficiency enhancement. Appl Energy (2016), http://dx.doi.org/10.1016/j.apenergy.2016.02.007

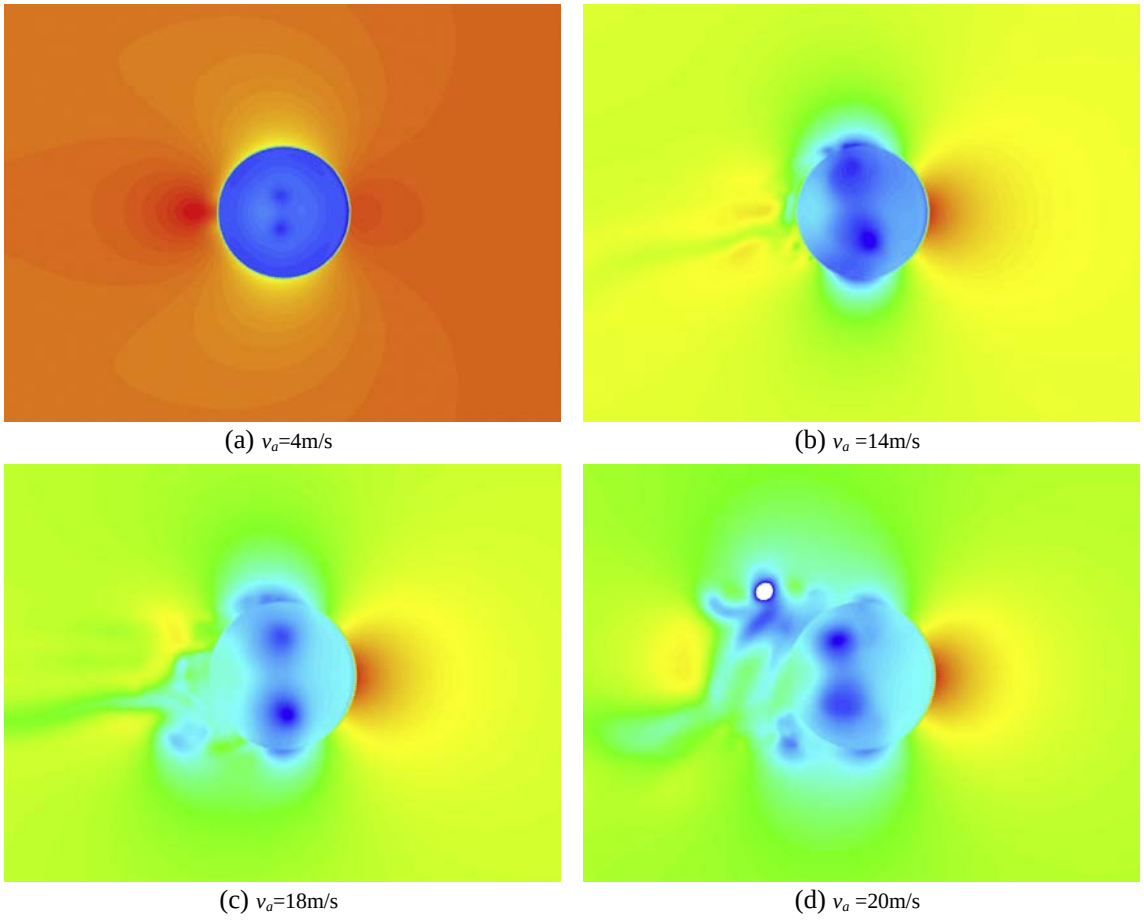

Fig. 6. Pressure contours at a cross plane of z = 14 m at different crosswind.

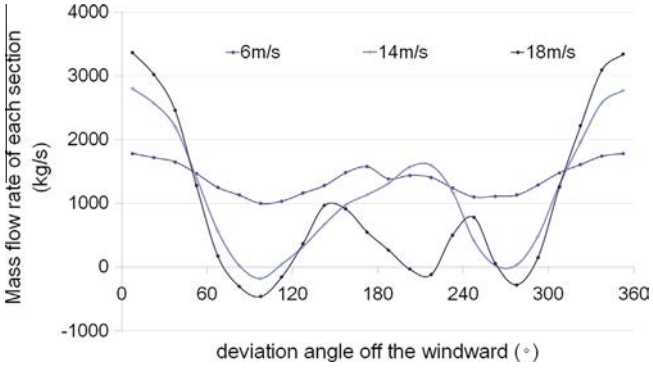

Fig. 7. Circumferential distribution of the air flow rate through radiator sections.

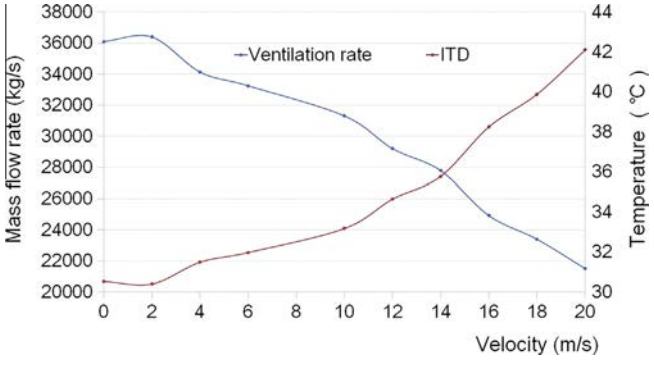

Fig. 8. The ventilation rate and ITD at different crosswind.

3.2. The cooling performance of a NDDCT with an enclosure

Based on the analyses of the flow field, pressure distribution, and Rrr of a NDDCT under crosswind condition from 0 to 20 m/s, a conceptual design of an enclosure arranged outside the radiator with an opening at the windward side is proposed to collect the upwind and increase the surrounding pressure outside the radiators at the side and back sections as described in Fig. 3. The flow fields of the vertical parting surface and the cross section inside the radiators with the enclosure at crosswind speed of 20 m/s are illustrated in Figs. 11 and 12 respectively. By comparing to the correspondent flow fields of the base NDDCT in Figs. 4 and 5, it can be easily drawn that the inner wall vortex and mainstream vortices are all weakened by the enclosure. What's more, the cross ventilation and flow out at the side section are both eliminated as shown in Fig. 12.

Fig. 13 illustrates the Rrr trends of the NDDCT with the enclosure under different crosswind conditions. By comparing to the Rrr trends of the base NDDCT shown in Fig. 10, the variation of the Rrr-radiator is obviously reduced under crosswind condition either in the favourable side or in the cooling performance degradation side, due to the improvement in the circumferential ventilation uniformity. The increment of Rrr-bottom under all crosswind conditions is obviously reduced as the weakening of the flow complexity in the bottom section as discussed in the last paragraph. However the increment of the Rrr-chamber is neither reduced

Please cite this article in press as: Wang W et al. The cooling performance of a natural draft dry cooling tower under crosswind and an enclosure approach to cooling efficiency enhancement. Appl Energy (2016), http://dx.doi.org/10.1016/j.apenergy.2016.02.007

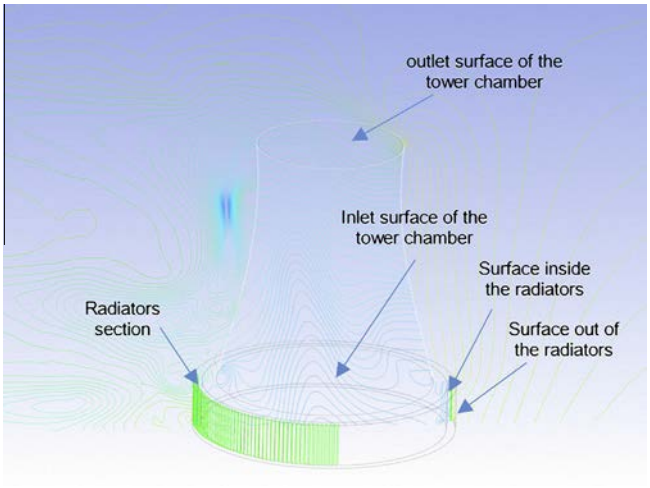

Fig. 9. The locations of the pressure surfaces selected.

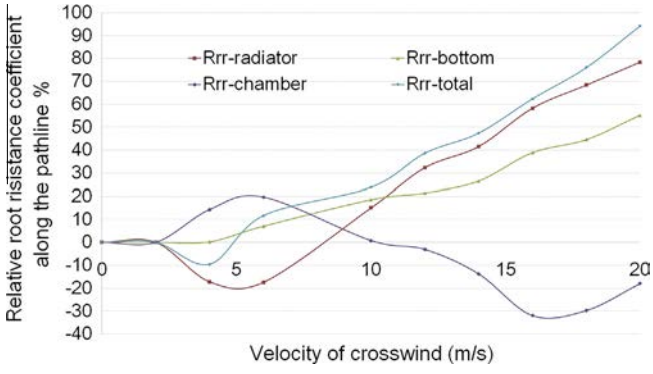

Fig. 10. Relative resistance coefficients between interest pressure surfaces under different approaches conditions.

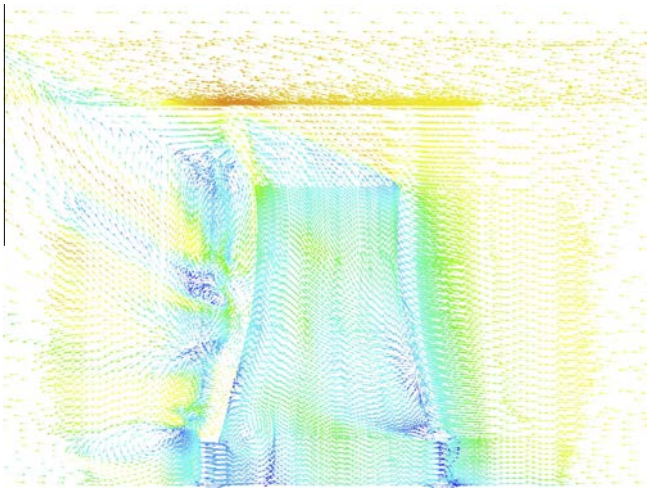

Fig. 11. The flow field of the vertical parting surface of the NDDCT with an enclosure at 20 m/s crosswind.

under low crosswind condition, nor transferred to be favourable way (negative value), which is mostly as the result of the weakening of the mainstream vortices without expanding the effective flow area in the plenum chamber.

A comparison between the circumferential ventilation rate distribution of a base NDDCT and a NDDCT with the enclosure at 16 m/s is shown in Fig. 14. It can be found that the ventilation rates

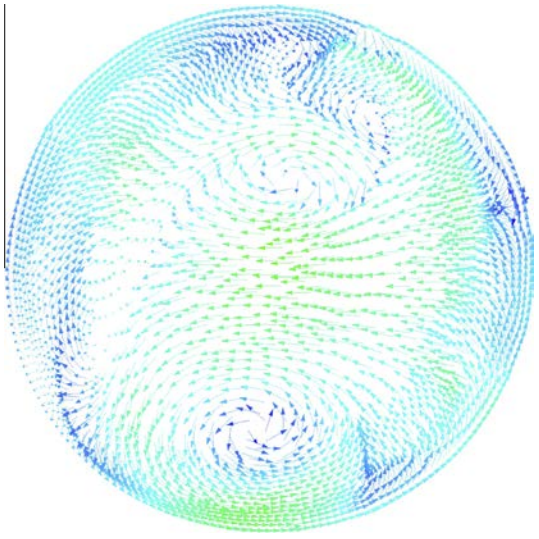

Fig. 12. The flow field of the cross section inside the radiators of the NDDCT with an enclosure.

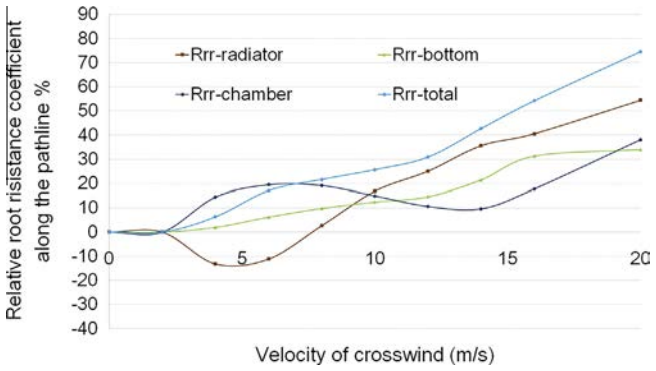

Fig. 13. Relative root resistance coefficients of each sections under enclosure condition.

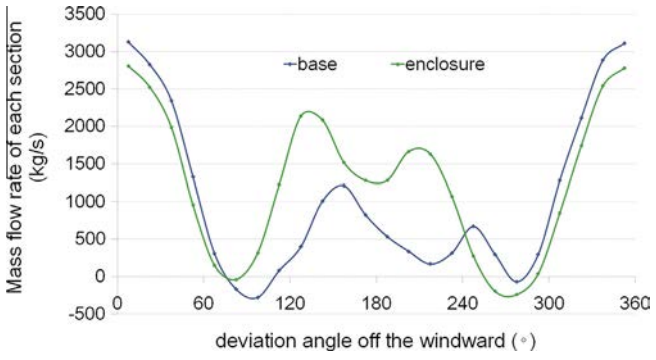

Fig. 14. Comparison of the circumferential ventilation distribution at 16 m/s crosswind.

at the windward sections are slightly reduced with the presence of the enclosure, while that at the leeward sections are greatly increased by the enclosure. That means the circumferential uniformity of the ventilation of the NDDCT is greatly improved by the enclosure.

The comparisons of the overall ventilation rate and ITD between a base NDDCT and a NDDCT with the enclosure are given in Figs. 15 and 16 respectively. It can be seen from Fig. 15 that the overall ventilation rate of the NDDCT with the enclosure barely changes when

Please cite this article in press as: Wang W et al. The cooling performance of a natural draft dry cooling tower under crosswind and an enclosure approach to cooling efficiency enhancement. Appl Energy (2016), http://dx.doi.org/10.1016/j.apenergy.2016.02.007

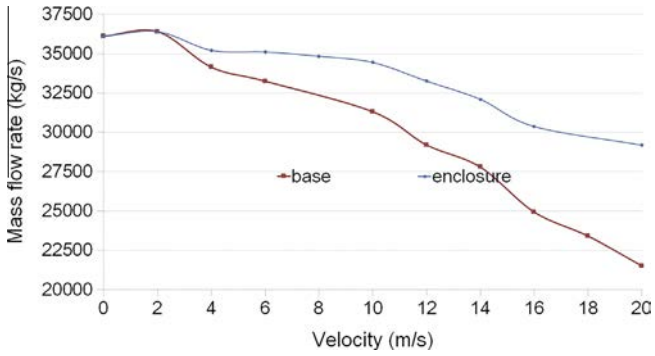

Fig. 15. The ventilation rate of the NDDCT with/without enclosure under different crosswind.

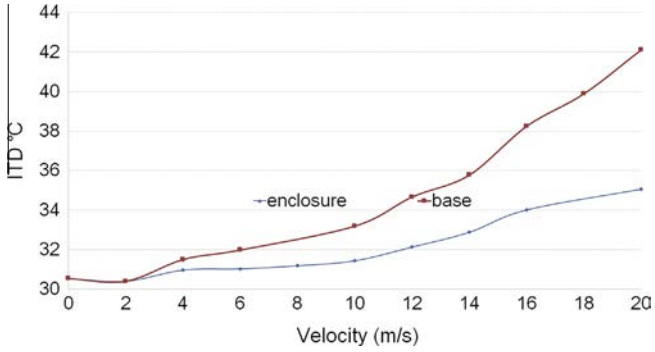

Fig. 16. The ITD of the NDDCT with/without enclosure under different crosswind.

crosswind velocity is less than 10 m/s, and slightly decreases at gale condition, then experiences the biggest ventilation degradation rate of 19%, with a 36% ventilation increment compared to the base NDDCT when the crosswind velocity is 20 m/s. Correspondingly, shown in Fig. 16, the ventilation rate behaves in an opposite way, namely the ITD of the NDDCT with the enclosure experiences a reduction of 7.05 °C compared to that of the base NDDCT at wind speed of 20 m/s. This is a great progress to the cooling performance of unit as it significantly reduces the energy consumption.

4. Conclusions

A CFD modelling for an in-service NDDCT of a 660 MW power plant is built and validated by experimental and design data. The characteristics of the air flow resistance at the radiators section is modelled based on the first order mechanism due to the low Reynolds number of the air flow between the fins of the radiator tubes, which is found to be critical to determine the cooling performance of the NDDCT.

Through investigating the flow field, pressure distribution, and relative resistance characteristic of the NDDCT under crosswind condition, the vortices stuck to the inner wall of the tower shell, the mainstream vortices, and the circumferential non-uniformity of the ventilation are found to be the main factors to degrade the cooling performance.

By adopting an enclosure outside the radiators, the circumferential non-uniformity and the complexity of the air flow inside the tower are greatly improved, leading to a large increment of the ventilation rate, and so as to a great enhancement of the cooling performance of the NDDCT, which is more obvious in gale condition. However, the proposed enclosure with a large size is only in the stage of conceptual design. It should be further validated or optimized with experiments or real application.

Acknowledgements

This research is supported by State Key Lab of Power Systems (SKLD13KZ05), Special Funds of the National Natural Science Foundation of China (No. L1522032), and the Consulting Project of Chinese Engineering Academy (No. 2015-ZCQ-06).

References

[1] Davies E, Kyle P, Edmonds JA. An integrated assessment of global and regional water demands for electricity generation to 2095. Adv Water Resour 2013;52:296–313.
[2] Calautit JK, Chaudhry HN, Hughes BR, Ghani SA. Comparison between evaporative cooling and a heat pipe assisted thermal loop for a commercial wind tower in hot and dry climatic conditions. Appl Energy 2013;101:740–55.
[3] Hanak DP, Biliyok C, Manovic V. Efficiency improvements for the coal-fired power plant retrofit with CO_2 capture plant using chilled ammonia process. Appl Energy 2015;151:258–72.
[4] Salazar JM, Diwekar U, Constantinescu E, Zavala VM. Stochastic optimization approach to water management in cooling-constrained power plants. Appl Energy 2013;112:12–22.
[5] Wei Q, Zhang B, Liu K, Du X, Meng X. A study of the unfavorable effects of wind on the cooling efficiency of dry cooling towers. J Wind Eng Ind Aerod 1995;54–55:633–43.
[6] Cui X, Lu X. Research on the economic characteristic and influence factors of cooling system. Inn Mongolia Petrochem 2013:121–2.
[7] Lu Y, Guan Z, Gurgenci H, Hooman K, He S, Bharathan D. Experimental study of crosswind effects on the performance of small cylindrical natural draft dry cooling towers. Energy Convers Manage 2015;91:238–48.
[8] Zhao S, Xu M, Zhang H, Guo F. Numerical simulation of the indirect air cooling tower layout optimization. Chinese J Hydrodyn 2013;28:197–202.
[9] Zhang X, Wang Q. Impact of side wind on the cooling performance of natural draft dry cooling tower. Electr Power 1999;32:34–6.
[10] Al-Waked R, Behnia M. The performance of natural draft dry cooling towers under crosswind: CFD study. Int J Energy Res 2004;28:147–61.
[11] Goudarzi MA. Proposing a new technique to enhance thermal performance and reduce structural design wind loads for natural drought cooling towers. Energy 2013;62:164–72.
[12] Yang LJ, Wu XP, Du XZ, Yang YP. Dimensional characteristics of wind effects on the performance of indirect dry cooling system with vertically arranged heat exchanger bundles. Int J Heat Mass Transf 2013;67:853–66.
[13] Zhao YB, Long G, Sun F, Li Y, Zhang C. Numerical study on the cooling performance of dry cooling tower with vertical two-pass column radiators under crosswind. Appl Therm Eng 2015;75:1106–17.
[14] Zhao Y, Sun F, Li Y, Long G, Yang Z. Numerical study on the cooling performance of natural draft dry cooling tower with vertical delta radiators under constant heat load. Appl Energy 2015;149:225–37.
[15] Chu CM. Use of chilton–colburn analogy to estimate effective plume chimney height of a forced draft, air-cooled heat exchanger. Heat Transf Eng 2006;27:81–5.
[16] Chu C, Rahman MM, Kumaresan S. Effect of cold inflow on chimney height of natural draft cooling towers. Nucl Eng Des 2012;249:125–31.
[17] Tang G, Su M, Fu S. Numerical study on flow field of a dry-cooling tower in a cross wind. Acta Aerodyn Sin 1997;15:328–36.
[18] Zhai Z, Tang G, Fu S, Zhu K. Experimental and numerical study of the influence of cross wind on the performance of natural draft dry-cooling tower. Therm Power Gener 1997:3–7.
[19] Zhai Z, Fu S, Zhu K. Comparison of flow characteristics and improving techniques in single and double dry cooling tower under cross wind. Acta Aerodyn Sin 1999;17:31–9.
[20] Zhang X, Zheng Y, Wang Q. Numerical analysis of the inner and outer flow field of an air-cooling tower. J Eng Therm Energy Power 2000;15:52–4.
[21] Goodarzi M. A proposed stack configuration for dry cooling tower to improve cooling efficiency under crosswind. J Wind Eng Ind Aerod 2010;98:858–63.
[22] Bergles AE. Air-cooled heat exchangers and cooling towers: thermal-flow performance evaluation and design. Mech Eng 2000;122:96.
[23] Zhai Z, Fu S. Improving cooling efficiency of dry-cooling towers under cross wind conditions by using wind-break methods. Appl Therm Eng 2006;26:1008–17.
[24] Fisher TS, Torrance KE. Experiments on chimney-enhanced free convection. J Heat Transf 1999;121:603–9.
[25] Chen L, Yang Z, Zou X, Yang S. The development of air-cooled power plant technology in China. J. Northeast Dianli Univ. 2012;32:38–42.
[26] Surface MO. System designs for dry cooling towers. Power Eng 1977;81:42–50.
[27] Du Preez AF, Kroger DG. Effect of wind on performance of a dry-cooling tower. Heat Recov Syst CHP 1993;13:139–46.
[28] Al-Waked R, Behnia M. The effect of windbreak walls on the thermal performance of natural draft dry cooling towers. Heat Transf Eng 2005;26:50–62.

Please cite this article in press as: Wang W et al. The cooling performance of a natural draft dry cooling tower under crosswind and an enclosure approach to cooling efficiency enhancement. Appl Energy (2016), http://dx.doi.org/10.1016/j.apenergy.2016.02.007

[29] Dai Z, Sun F, Wang H, Gao M. Performance evaluation and its comparison of cooling towers before and after the installation of air deflectors. Electr Power 2009:24–7.
[30] Wang K. Research on flow resistance of inlet air and performance optimization of natural draft counterflow wet cooling tower with air deflectors. Shangdong University; 2009.
[31] Zhao Y, Sun F, Wang K, Chen Y, Gao M, Wang H, et al. Numerical analysis of the cooling performance of wet cooling tower with cross wall. Proc CSEE 2009;29:6–13.
[32] Chen Y, Sun F, Gao M, Zhao Y, Shi Y. Experimental study of cross walls effect on the performance of wet cooling towers. Proc CSEE 2012;32:28–34.
[33] Lu Y, Guan Z, Gurgenci H, Zou Z. Windbreak walls reverse the negative effect of crosswind in short natural draft dry cooling towers into a performance enhancement. Int J Heat Mass Transf 2013;63:162–70.
[34] Goodarzi M, Keimanesh R. Heat rejection enhancement in natural draft cooling tower using radiator-type windbreakers. Energy Convers Manage 2013;71:120–5.
[35] Goodarzi M, Ramezanpour R. Alternative geometry for cylindrical natural draft cooling tower with higher cooling efficiency under crosswind condition. Energy Convers Manage 2014;77:243–9.
[36] Calautit JK, Hughes BR. A passive cooling wind catcher with heat pipe technology: CFD, wind tunnel and field-test analysis. Appl Energy 2016;162:460–71.
[37] Lu Y, Wang S, Shan K. Design optimization and optimal control of grid-connected and standalone nearly/net zero energy buildings. Appl Energy 2015;155:463–77.
[38] Fluent. Ansys Fluent theory guide. 14.0 ed: ANSYS, INC; 2011.
[39] Yang LJ, Chen L, Du XZ, Yang YP. Effects of ambient winds on the thermo-flow performances of indirect dry cooling system in a power plant. Int J Therm Sci 2013;64:178–87.
[40] Xu C, Dowd PA, Tian ZF. A simplified coupled hydro-thermal model for enhanced geothermal systems. Appl Energy 2015;140:135–45.
[41] Barigozzi G, Perdichizzi A, Ravelli S. Performance prediction and optimization of a waste-to-energy cogeneration plant with combined wet and dry cooling system. Appl Energy 2014;115:65–74.
[42] Barigozzi G, Perdichizzi A, Ravelli S. Wet and dry cooling systems optimization applied to a modern waste-to-energy cogeneration heat and power plant. Appl Energy 2011;88:1366–76.
[43] Ko T, Ting K. Optimal Reynolds number for the fully developed laminar forced convection in a helical coiled tube. Energy 2006;31:2142–52.
[44] Hajmohammadi MR, Lorenzini G, Shariatzadeh OJ, Biserni C. Evolution in the design of V-shaped highly conductive pathways embedded in a heat-generating piece. J Heat Transf ASME 2015;137:61001.
[45] Hajmohammadi MR, Nourazar SS, Campo A, Poozesh S. Optimal discrete distribution of heat flux elements for in-tube laminar forced convection. Int J Heat Fluid Flow 2013;40:89–96.
[46] Hajmohammadi MR, Maleki H, Lorenzini G, Nourazar SS. Effects of Cu and Ag nano-particles on flow and heat transfer from permeable surfaces. Adv Powder Technol 2015;26:193–9.
[47] Hajmohammadi M, Moulod M, Shariatzadeh OJ, Nourazar S. Essential reformulations for optimization of highly conductive inserts embedded into a rectangular chip exposed to a uniform heat flux. Proc Inst Mech Eng Part C: J Mech Eng Sci 2014;228:2337–46.
[48] Najafi H, Najafi B, Hoseinpoori P. Energy and cost optimization of a plate and fin heat exchanger using genetic algorithm. Appl Therm Eng 2011;31:1839–47.
[49] Reuter HCR, Kroeger DG. Computational fluid dynamics analysis of cooling tower inlets. J Fluids Eng – Trans ASME 2011:133.

Please cite this article in press as: Wang W et al. The cooling performance of a natural draft dry cooling tower under crosswind and an enclosure approach to cooling efficiency enhancement. Appl Energy (2016), http://dx.doi.org/10.1016/j.apenergy.2016.02.007